

1

Supplementary Material

2

Aaron

3

04 August, 2021

4

Data availability

5 All data is publically available and published by the queensland government. Individual serological and PCR
6 data is available at the following location:

7 <https://www.data.qld.gov.au/dataset/hendra-virus-infection-in-australian-black-flying-foxes-pteropus-alecto>

9 Under-roost data can be obtained at the following location:

10 <https://www.data.qld.gov.au/dataset/hev-infection-flying-foxes-eastern-australia>

Model description

Discrete time model equations

13 The age structured viral dynamics model, with all potential transitions is stated in the equations below,
14 with parameters corresponding to table 1 in the main text, transitions between states occurs in discrete
15 time ($t \rightarrow t + 1$), in each model discrete time setps (t) are set to 0.25 days.

16

$$17 S_J(t+1) = S_J(t) + 2b(t)(S_F(t) + I_F(t)) - (\omega_m + m_j \frac{N}{\kappa} + \beta(I_S A(t) + I_J(t) + I_F(t) + I_M(t)))S_J(t) + \omega R_J(t)$$

$$18 S_{SA}(t+1) = S_{SA}(t) + \omega_m(S_J(t) + Ma) - (\mu + m_j \frac{N}{\kappa} + \beta(I_S A(t) + I_J(t) + I_F(t) + I_M(t)))S_{SA}(t) + \omega R_{SA}(t)$$

$$19 S_M(t+1) = S_M + (t)\mu \frac{S_{SA}}{2} - (m \frac{N}{\kappa} + \beta(I_S A(t) + I_J(t) + I_F(t) + I_M(t)))S_M(t)I_M(t) + \omega R_M(t)$$

$$20 S_F(t+1) = S_F(t) + \mu \frac{S_{SA}}{2} - (m \frac{N}{\kappa} + \beta(I_S A(t) + I_J(t) + I_F(t) + I_M(t)))S_F(t) + \omega R_F(t)$$

$$21 L_J(t+1) = L_J(t) - (\omega_m + m_j \frac{N}{\kappa} + \epsilon)L_J + \rho I_J$$

$$22 L_{SA}(t+1) = L_{SA}(t) + \omega_m L_J(t) - (m_j \frac{N}{\kappa} + \epsilon)L_{SA}(t) + \rho L_{SA}(t)$$

$$23 L_M(t+1) = L_M(t) + \mu \frac{L_{SA}}{2} - (m_j \frac{N}{\kappa} + \epsilon)L_M(t) + \rho L_M(t)$$

$$24 L_F(t+1) = L_F(t) + \mu \frac{L_{SA}}{2} - (m_j \frac{N}{\kappa} + \epsilon)L_F(t) + \rho L_F(t)$$

$$25 I_J(t+1) = I_J(t) - (\omega_m + m_j \frac{N}{\kappa} + \gamma + \rho)I_J + \beta(I_S A(t) + I_J(t) + I_F(t) + I_M(t))S_J + \epsilon L_J$$

$$26 I_{SA}(t+1) = I_{SA}(t) + \omega_m I_J - (\mu \frac{S_{SA}}{2} + m_j \frac{N}{\kappa} + \gamma + \rho)I_{SA} + \beta(I_S A(t) + I_J(t) + I_F(t) + I_M(t))S_{SA} + \epsilon L_{SA}$$

$$27 I_F(t+1) = I_F(t) + \mu \frac{I_{SA}}{2} - (m \frac{N}{\kappa} \gamma + \rho)I_F(t) + \beta(I_F(t) + I_M(t))S_F(t) + \epsilon L_F(t)$$

$$28 I_M(t+1) = I_M(t) + \mu \frac{I_{SA}}{2} - (m \frac{N}{\kappa} + \gamma + \rho)I_M(t) + \beta(I_M(t) + I_F(t))S_M(t) + \epsilon L_M(t)$$

$$29 R_J(t+1) = R_J(t) - (\omega_m + m_j \frac{N}{\kappa} + \omega)R_J(t)$$

30 $R_S A(t+1) = R_S A(t) + \omega_m R_J(t) - (m_j \frac{N}{\kappa} + \omega) R_S A(t)$
 31 $R_M(t+1) = R_M(t) + \mu \frac{R_S A(t)}{2} - (m \frac{N}{\kappa} + \omega) R_M(t) + \gamma I_M(t)$
 32 $R_F(t+1) = R_F(t) + \mu \frac{R_S A(t)}{2} - (m \frac{N}{\kappa} + \omega) R_F(t) + \gamma I_F(t)$
 33 $M_a(t+1) = M_a(t) + 2b(R_F(t) + L_F(t)) - (\omega_m + m_j \frac{N}{\kappa}) M_a(t)$

34
35

36 Births occur in seasonal pulses, as previously described (Peel et al. 2014), with timing, amplitude and
37 seasonality derived from three parameters in a modified Gaussian function.

$$b(t) = c \exp^{s \cos^2(\pi t - \phi)} \quad (1)$$

β is derived from a rearrangement of equation (2) in the main text, here N is considered an upper limit to the population, thus N is equal to the carrying capacity κ :

$$\beta = R_0 \left(\frac{(\epsilon + m)(\gamma + m + \rho) - \epsilon \rho}{N(\epsilon + m)} \right) \quad (2)$$

38
39

40 Stochastic transitions between states

41 Movement between states at each discrete time-step (set as 0.25 days) for individuals is a stochastic process,
42 using a combination of binomial, and multinomial distributions where multiple transition possibilities occur.
43 e.g. for bats exiting the variable state R , transitions will occur with the following steps:

- 44 • The total number of individuals transitioning between states is determined by first summing all of the
45 rates of exiting a current state, e.g. $(R \rightarrow \text{exit}) = \omega + \frac{N}{\kappa}$.
- 46 • We then convert the sum of rates to a probability for each possible transition occurring during a single
47 time-step, e.g. for a rate x , the equivalent probability of transition in one time-step is $p = 1 - e^{-x}$,
48 thus $Pr(R \rightarrow \text{exit}) = 1 - e^{-(R \rightarrow \text{exit})}$
- 49 • For each individual, a random draw from a binomial distribution is then performed at each time-step
50 to obtain the number of individuals exiting R e.g. $R_e = \text{bin}(R, Pr(R \rightarrow \text{exit}))$.
- The relative probabilities are then computed for transition to each of the potential states

$$Pr(R \rightarrow S) = \frac{\omega}{m \frac{N}{\kappa} + \omega} \quad (3)$$

and

$$Pr(R \rightarrow \text{death}) = \frac{m \frac{N}{\kappa}}{m \frac{N}{\kappa} + \omega} \quad (4)$$

- 51 • A multinomial distribution is used with each probability to determine the destination of each
52 individual $M(R_e, Pr(R \rightarrow S), Pr(R \rightarrow \text{death}))$

53

54 **Model fitting**

55 Our models are considered state-space (hidden Markov) models, with observations k and hidden state vari-
 56 ables Z at time t and we seek to identify an unbiased estimate of the likelihood value, (also known as a
 57 marginal likelihood) $pr(k|\theta)$, by essentially “marginalising out” (Z). Here we do this using a particle markov
 58 chain monte carlo (pMCMC) algorithm. Which combines a particle filter as an unbiased estimator of the
 59 marginal likelihood value, and an MCMC acceptance/rejection algorithm (Andrieu, Doucet, and Holenstein
 60 2010).

61 **pMCMC generic example**

62 Particle filters act as an unbiased estimator of marginal likelihood by applying a form of importance re-
 63 sampling, to generate an approximate sample from, and make inferences about an unobserved Markov
 64 process (Smith 2013). They are becoming popular in disciplines where state-space models are common such
 65 as ecology and epidemiology (Kantas et al. 2015; Peters, Hosack, and Hayes 2010; Knape and De Valpine
 66 2012; Fasiolo et al. 2016; Sheinson, Niemi, and Meiring 2014).

67 In brief, the marginal likelihood $pr(k|\theta)$ for the observed data k , the hidden state Z and the parameter
 68 vector θ is considered the joint posterior probability $pr(k|Z, \theta) * p(Z|\theta)$. Using Monte-Carlo approximation
 69 for $p(k|\theta)$, a particle filter with j particles which have the possible trajectories/evolution of Z_j , the marginal
 70 likelihood can be considered as $pr(k|\theta) \approx \sum_j pr(k|Z_j, \theta) * pr(Z_j|\theta)$.

71 To run the particle filter algorithm requires the following steps:

1. Initialise the particles with equal weights.

$$Z_j \sim pr(Z_j|\theta) \quad (5)$$

$$w_j = \frac{1}{J}$$

72
73

2. For each particle j at time t , simulate the initial conditions at the first observed data point.

$$Z_{jt} \sim pr(Z_{jt}|Z_j, \theta) \quad (6)$$

74
75

3. Calculate a probability weighting for each particle based on the results of the simulation and the observed data.

$$w_{jt} = pr(k_t|Z_j, \theta) \quad (7)$$

76
77

4. The marginal likelihood for this data point can be considered the average of each particle weighting.

$$p(k_t|\theta) = \frac{1}{J} \sum_J w_{jt} \quad (8)$$

78
79

5. Normalise the weightings $\frac{w_{jt}}{\sum_J w_{jt}}$, resample with replacement each particle based on their weighting and simulate forward to the next observed data point.

$$Z_{jt+1} \sim pr(Z_{jt+1}|Z_t, \theta) \quad (9)$$

80

81

Repeat steps 3 to 5 for all observed data, an estimate for the total marginal likelihood value can be considered the product of the average particle weights at each observed timepoint.

$$\mathcal{L}(\theta|k_{1:n}) = \prod_{t=1}^n \left(\frac{1}{J} \sum_{j=1}^J w_{jt} \right) \quad (10)$$

82

83

84 This marginal likelihood value is then used in a traditional MCMC algorithm, in this instance Metropolis-
85 Hastings, where rejection or acceptance of a parameter proposal is based on the current and previous marginal
86 likelihood values.

87 Model fitting with pMCMC to Boonah bat data

88 To fit the model with pMCMC to our observed data, we developed a likelihood function which incorporated
89 the three unique longitudinal data-types; Individual serology for Hendra virus antibodies, individual PCR
90 of urine for Hendra virus RNA, and under roost PCR of urine for Hendra virus RNA.

- 91 • *Firstly, we consider the observed data:*

92 If the sampling time points are $i_1 \dots i_n$, the number of individual samples through time are $N_{i \dots n}$ of
93 which $k_{i \dots n}^p$ are PCR positive and $k_{i \dots n}^s$ are seropositive, the number of under-roost urine samples is
94 $N_{i \dots n}^u$ of which $k_{i \dots n}^u$ are PCR positive.

- 95 • *Secondly, the hidden state:*

96 If the system state of the model at each time point is $Z_{i \dots n}$, the transition probability density function
97 for Z from the stochastic model, conditioned on the parameters θ , is $pr(Z_i|Z_{i-1}, \theta)$.

98 Below we define how each data type contributes to the likelihood function in detail:

Table 1: Parameter and variable descriptions for supplementary materials

Parameter	Unit	Prior	Description
S	Individual bats	-	Susceptible bats
I	Individual bats	-	Infectious bats
R	Individual bats	-	Recovered bats
L	Individual bats	-	Latently infected bats
N	Individual bats	-	Total bat population
J	Individual bats	-	Juveniles
M_a	Individual bats	-	Maternally immune juveniles
S_A	Individual bats	-	Sub-adults
F	Individual bats	-	Adult females
M	Individual bats	-	Adult males
θ	-	-	Parameter vector
Z	-	-	System state
z	-	-	Vector of simulated individual bat states
ζ_s	-	0-1	Individual serology coefficient
ζ_p	-	0-1	Individual PCR coefficient
ζ_u	-	0-1	Under roost PCR coefficient
k^s	Individual bats	-	Observed individual seropositive bats
k^p	Individual bats	-	Observed individual PCR positive bats
k^u	Individual bats	-	Predicted no. positive bats contributing to pooled under roost samples
k	-	-	Vector of observed individual bat states
N^u	-	-	Number of pooled under-roost samples (mean)
p	$\frac{I\zeta_u}{N}$	-	Probability of bat being positive (infection prevalence)
P_t	$1 - (1 - p)^d$	-	Probability of pooled sample being positive
O_u	-	>0	Overdispersion parameter for under roost data
d	-	1-30	Number of bats contributing to each pooled under roost sample
T_i	-	-	Pooled under roost sample test state

¹ Informative priors are based on normal distributions and are shown with 95% credible intervals in brackets, uninformative priors use a uniform distribution and are shown as a minimum and maximum value

101 ***Individual serological and PCR of urine samples***

102 In the observed data, individual bats are found to be in all four empirical states of serological and PCR
 103 positivity:

- 104 • PCR positive and seropositive ($k^{P^+S^+}$)
 105 • PCR negative and seropositive ($k^{P^-S^+}$)
 106 • PCR positive and seronegative ($k^{P^+S^-}$)
 107 • PCR negative and seronegative ($k^{P^-S^-}$)

108 Logically, a relationship between the PCR and serology states is likely and so we consider a joint conditional
 109 probability function rather than treating the data as independent. Transitory states and test detection
 110 failure are also considered by fitting the coefficients ζ_s and ζ_p , which are bounded between 0 and 1. Thus,
 111 the simulated implementation of each observed empirical state are as follows:

- 112 • $k^{P^+S^+}$: Bats are assumed to be in the I state of the model and are equivalent to the number of I state
 113 bats proportionate to the value of the coefficients; $z^{P^+S^+} = I\zeta_p\zeta_s$
 114 • $k^{P^-S^+}$: Bats are assumed to be in either the L or R states of the models, or in the I state of the model;
 115 $z^{P^-S^+} = (I + L + R)\zeta_s(1 - \zeta_p)$
 116 • $k^{P^+S^-}$: Bats are considered to be in the I state of the model; $z^{P^+S^-} = I(1 - \zeta_s)\zeta_p$
 117 • $k^{P^-S^-}$: Bats are assumed to be in the S state of the models or in the I state; $z^{P^-S^-} = I(1 - \zeta_s)(1 - \zeta_p) + S$

118 If k is a vector of the observed counts of bats in each empirical state, $k = (k^{P^+S^+}, k^{P^-S^+}, k^{P^+S^-}, k^{P^-S^-})$,
 119 z is a vector of the simulated prevalences of each state $z = (z^{P^+S^+}, z^{P^-S^+}, z^{P^+S^-}, z^{P^-S^-})$ and N is the
 120 total observed bats, we can then propose a joint probability function based on a multinomial distribution,
 121 $pr(k^p, k^s | Z, N)$.

$$pr(k^p, k^s | Z) = \frac{N!}{\prod_{j=1}^4 k_j!} \prod_{j=1}^4 z_j^{k_j} \quad (11)$$

122 ***Pooled under roost samples***

If the probability of at least one bat within a pooled urine sample of d individuals being PCR positive for virus RNA can be considered $P_t = 1 - (1 - p)^d$, where p is the probability of each individual bat contributing to a pool being positive (Chiang and Reeves 1962). The result of PCR testing on a pooled sample (T_i) will be one of two states, with the following probabilities:

$$T_i = \begin{cases} \text{positive} = 1 - (1 - p)^d \\ \text{negative} = (1 - p)^d \end{cases} \quad (12)$$

123 Therefore, assuming that any one under-roost sample comes from d bats with a prevalence of p , considering
 124 the model state $Z(t)$, we aim to identify the likelihood of the contribution of positive under-roost samples at
 125 time (t) given (from the predicted GAM values) the number of samples $N^u(t)$, of which $k^u(t)$ were positive,
 126 $pr(k^u | N^u, Z)$. As the predicted values from the GAM are for prevalence, the total number of bats ($N^u(t)$)
 127 was considered the mean number of samples collected on each sampling occasion.

128 Due to the nature and challenges of field-sampling, under-roost data is likely to contain a degree of overdisper-
 129 sion, as it is highly exposed to external factors which are difficult to account for in study design. Therefore,
 130 the probability is unlikely to follow a standard binomial distribution, where the variance is defined by the
 131 mean. To account for this, we used a probability function based around a beta-binomial distribution, which

¹³² allows for an additional variance parameter to be fitted to account for any overdispersion in the observations.
¹³³ A beta-binomial distribution, is a binomial distribution such $pr(k^u|N^u, Z)$ would be:

$$pr(k^u|N^u, Z) = \binom{N^u}{k^u} p_t^{k^u} (1 - p_t)^{N^u - k^u} \quad (13)$$

¹³⁴ However, p_t is not constant and is generated from a beta distribution, which takes two shape parameters α
¹³⁵ and β , $beta(\alpha, \beta)$ thus;

$$pr(k^u|N^u, Z) = \frac{\binom{N^u}{k^u} beta(k^u + O_u p, N^u - k^u + O_u(1 - p_t))}{beta(O_u p, O_u(1 - p_t))} \quad (14)$$

¹³⁶ Here, O_u accounts for overdispersion in the data, and the prevalence of infectious bats p in p_t is derived from
¹³⁷ the model state $Z(t)$ as $\frac{I(t)\zeta_u}{N(t)}$, where ζ_u is a fitted coefficient accounting for detection failure.

¹³⁸ As there is no precise measure of exact bat numbers contributing to a pooled sample, d is a fitted parameter
¹³⁹ with a prior based on expert knowledge and estimates from the field. For simplicity, only one value of d is
¹⁴⁰ derived for all pools on a single sampling occasion, assuming that each pooled sample on average has the
¹⁴¹ same number of bats contributing. We also assume that there is no effect of pooling on the diagnostic tests,
¹⁴² and any that does occur should be primarily accounted for by the ζ_u coefficient.

¹⁴³ ***full likelihood function***

¹⁴⁴ Considering the above, and the sampling time points (i), we can define the full likelihood function as:

$$\mathcal{L}(\theta|N, N^u, k^{(s,p,u)}) = pr(\theta) * \prod_{i=1}^{16} pr(k_i^s, k_i^p|N_i, Z_i) * pr(k_t^u|N_i^u, Z_i) \quad (15)$$

¹⁴⁵
¹⁴⁶

¹⁴⁷ **Initial conditions**

¹⁴⁸ Starting parameters are estimated by running a Metropolis-Hastings MCMC algorithm with a deterministic
¹⁴⁹ version of the model for 50,000 iterations with a 10,000 iteration burn-in. The median parameter set from
¹⁵⁰ each posterior distribution was then used in the pMCMC.

¹⁵¹ Initial conditions for the bat population are derived from the carrying capacity parameter (κ). A population
¹⁵² equal to the carrying capacity is first assumed and this is then split into demographic compartments as
¹⁵³ follows:

$$N = \kappa \quad (16)$$

$$b = (\omega_m + m_j) \frac{m_j + \mu}{\omega_m} \quad (17)$$

$$S_F = 0.5 \left(\frac{N}{\frac{1+m}{\mu} + \frac{b}{\omega_m + m_j}} \right) \quad (18)$$

$$S_M = 0.5 \left(\frac{N}{\frac{1+m}{\mu} + \frac{b}{\omega_m + m_j}} \right) \quad (19)$$

$$S_S A = (S_F + S_M) \frac{m}{mu} \quad (20)$$

$$S_J = N - S_M - S_F - S_S A \quad (21)$$

¹⁵⁴ Infectious and exposed individuals are added as 5% of the population and the model is run for 50 years to
¹⁵⁵ reach an equilibrium before fitting to the first data point.

156 **Further results**

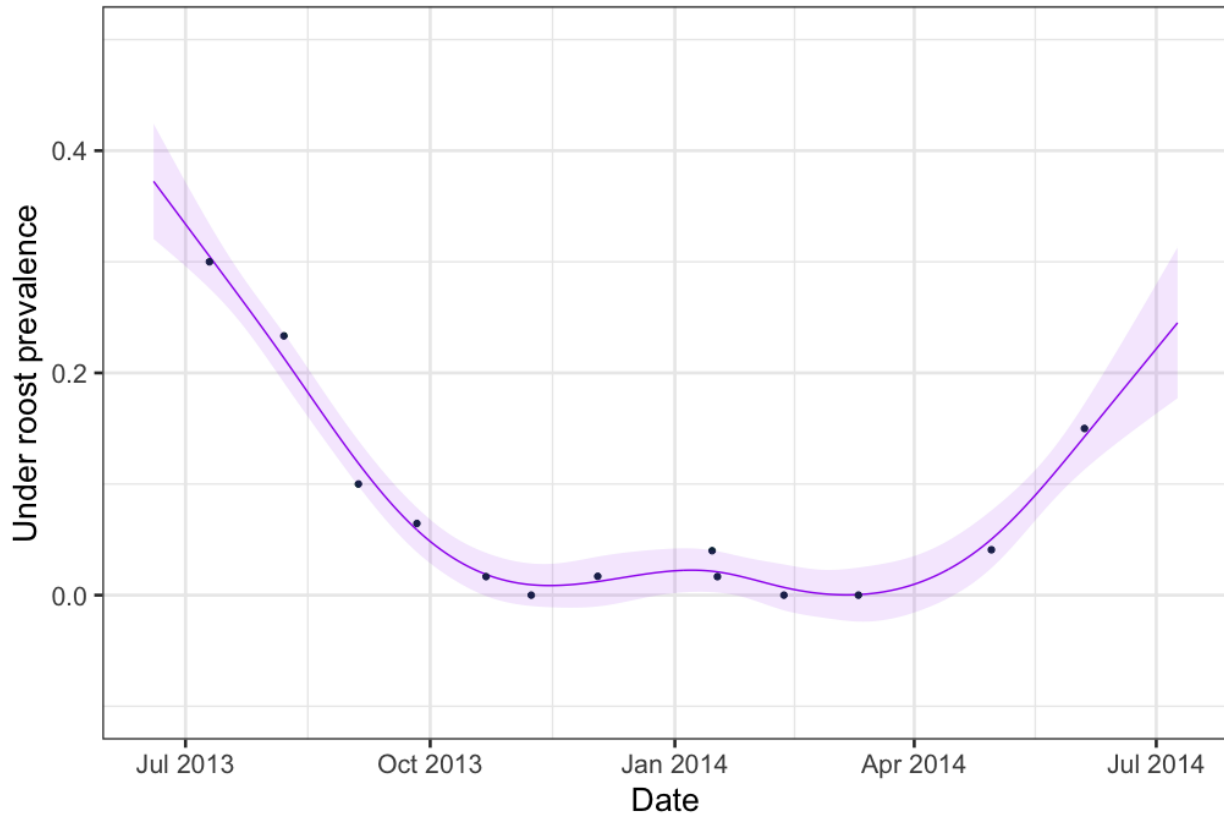


Figure 1: General Additive Model (GAM) fitted to the prevalence of samples PCR positive for Hendra virus RNA from pooled under-roost urine collections. Dark blue points are the observed values, the fitted GAM is shown in purple with 95 % confidence intervals. Predicted values from the GAM at corresponding time-points of individual urine and serological samples were taken for use in the rest of the study

Table 2: Model 1

Parameter	Prior	Posterior
γ	1 day - 10 years	0 (0-0) year ⁻¹
ρ	1 day - 10 years	2.111 (0.173-9.397) year ⁻¹
ϵ	1 day - 10 years	0.216 (0.1-17.947) year ⁻¹
m	0.186 (0.088-0.284) year ⁻¹	0.138 (0.05-0.231) year ⁻¹
m_j	0.500 (0.360-0.639) year ⁻¹	0.458 (0.326-0.588) year ⁻¹
c	-	8.309 (2.892-14.787)
s	130 (111-150)	128.813 (100.196-156.914)
ϕ	7.180 (6.787-7.571)	7.284 (7.063-7.405)
ω	1 day - 10 years	0 (0-0) year ⁻¹
ω_m	1.800 (1.41-2.19) year ⁻¹	1.792 (1.405-2.176) year ⁻¹
R_0	> 1	2.415 (1.014-3.501)
d	1-30	5.905 (0.005-25.22)
ζ_s	0-1	0.925 (0.839-0.989)
ζ_p	0-1	0.252 (0.03-0.604)
ζ_u	0-1	0.181 (0.015-0.744)
κ	4000 (2025-7867)	3985.015 (2042-7962)
c_ν	1	1
s_ν	-	0 (0-0)
ϕ_ν	-	0 (0-0)

¹ Table for model 1, SILI with no maternal immunity and no seasonal force, posterior estimates, 95% credible intervals are shown in brackets, model corresponds to model 1 in table SM1

Table 3: Model 2

Parameter	Prior	Posterior
γ	1 day - 10 years	$0 (0-0) \text{ year}^{-1}$
ρ	1 day - 10 years	$8.577 (0.153-33.651) \text{ year}^{-1}$
ϵ	1 day - 10 years	$0.526 (0.1-279.254) \text{ year}^{-1}$
m	$0.186 (0.088-0.284) \text{ year}^{-1}$	$0.198 (0.098-0.293) \text{ year}^{-1}$
m_j	$0.500 (0.360-0.639) \text{ year}^{-1}$	$0.508 (0.375-0.644) \text{ year}^{-1}$
c	-	$13.357 (5.367-22.035)$
s	$130 (111-150)$	$130.213 (99.824-160.113)$
ϕ	$7.180 (6.787-7.571)$	$7.179 (6.981-7.38)$
ω	1 day - 10 years	$0 (0-0) \text{ year}^{-1}$
ω_m	$1.800 (1.41-2.19) \text{ year}^{-1}$	$1.799 (1.429-2.184) \text{ year}^{-1}$
R_0	> 1	$8.108 (1.562-138.34)$
d	$1-30$	$11.428 (0.098-27.055)$
ζ_s	$0-1$	$0.807 (0.624-0.978)$
ζ_p	$0-1$	$0.526 (0.023-0.768)$
ζ_u	$0-1$	$0.177 (0.003-0.834)$
κ	$4000 (2025-7867)$	$3901.749 (2000-7379)$
c_ν	1	1
s_ν	-	$0 (0-0)$
ϕ_ν	-	$0 (0-0)$

¹ Table for model 2, SILI with maternal immunity and no seasonal force, posterior estimates, 95% credible intervals are shown in brackets, model corresponds to model 2 in table SM1

Table 4: Model 3

Parameter	Prior	Posterior
γ	1 day - 10 years	0 (0-0) year ⁻¹
ρ	1 day - 10 years	31.157 (6.412-362.243) year ⁻¹
ϵ	1 day - 10 years	7.823 (0.541-229.087) year ⁻¹
m	0.186 (0.088-0.284) year ⁻¹	0.137 (0.042-0.23) year ⁻¹
m_j	0.500 (0.360-0.639) year ⁻¹	0.449 (0.323-0.581) year ⁻¹
c	-	8.099 (2.321-14.086)
s	130 (111-150)	129.634 (103.189-159.768)
ϕ	7.180 (6.787-7.571)	7.261 (7.065-7.369)
ω	1 day - 10 years	0 (0-0) year ⁻¹
ω_m	1.800 (1.41-2.19) year ⁻¹	1.788 (1.396-2.172) year ⁻¹
R_0	> 1	2.414 (1.033-6.49)
d	1-30	7.617 (0.009-23.679)
ζ_s	0-1	0.917 (0.81-0.984)
ζ_p	0-1	0.365 (0.095-0.758)
ζ_u	0-1	0.346 (0.014-0.919)
κ	4000 (2025-7867)	4037.034 (2173-8147)
c_ν	1	1
s_ν	-	4.226 (1.971-22.087)
ϕ_ν	-	2.677 (0-3.089)

¹ Table for model 3, SILI with maternal immunity and no seasonal force, posterior estimates, 95% credible intervals are shown in brackets, model corresponds to model 3 in table SM1

Table 5: Model 4

Parameter	Prior	Posterior
γ	1 day - 10 years	0 (0-0) year ⁻¹
ρ	1 day - 10 years	122.328 (39.264-362.243) year ⁻¹
ϵ	1 day - 10 years	9.786 (2.148-57.016) year ⁻¹
m	0.186 (0.088-0.284) year ⁻¹	0.179 (0.089-0.266) year ⁻¹
m_j	0.500 (0.360-0.639) year ⁻¹	0.493 (0.351-0.628) year ⁻¹
c	-	11.626 (5.168-18.815)
s	130 (111-150)	130.361 (102.563-160.068)
ϕ	7.180 (6.787-7.571)	7.165 (6.979-7.377)
ω	1 day - 10 years	0 (0-0) year ⁻¹
ω_m	1.800 (1.41-2.19) year ⁻¹	1.772 (1.392-2.176) year ⁻¹
R_0	> 1	2.671 (1.098-5.53)
d	1-30	12.356 (0.992-27.422)
ζ_s	0-1	0.921 (0.832-0.99)
ζ_p	0-1	0.622 (0.335-0.839)
ζ_u	0-1	0.454 (0.09-0.955)
κ	4000 (2025-7867)	4052.089 (2178-8551)
c_ν	1	1
s_ν	-	3.437 (2.247-4.928)
ϕ_ν	-	0.027 (0-0.093)

¹ Table for model 4, SILI with maternal immunity and seasonal force, posterior estimates, 95% credible intervals are shown in brackets, model corresponds to model 4 in table SM1

Table 6: Model 5

Parameter	Prior	Posterior
γ	1 day - 10 years	3.428 (0.993-5.346) year ⁻¹
ρ	1 day - 10 years	0 (0-0) year ⁻¹
ϵ	1 day - 10 years	0 (0-0) year ⁻¹
m	0.186 (0.088-0.284) year ⁻¹	0.236 (0.136-0.32) year ⁻¹
m_j	0.500 (0.360-0.639) year ⁻¹	0.537 (0.408-0.68) year ⁻¹
c	-	17.282 (9.171-26.596)
s	130 (111-150)	130.872 (101.952-157.989)
ϕ	7.180 (6.787-7.571)	7.172 (6.996-7.334)
ω	1 day - 10 years	0 (0-0) year ⁻¹
ω_m	1.800 (1.41-2.19) year ⁻¹	1.832 (1.467-2.228) year ⁻¹
R_0	> 1	117.292 (46.35-149.935)
d	1-30	10.826 (1.52-27.492)
ζ_s	0-1	0.918 (0.82-0.987)
ζ_p	0-1	0.51 (0.324-0.624)
ζ_u	0-1	0.313 (0.054-0.854)
κ	4000 (2025-7867)	4057.727 (2168-7962)
c_ν	1	1
s_ν	-	0 (0-0)
ϕ_ν	-	0 (0-0)

¹ Table for model 5, SIR with no seasonal force, posterior estimates, 95% credible intervals are shown in brackets, model corresponds to model 5 in table SM1

Table 7: Model 6

Parameter	Prior	Posterior
γ	1 day - 10 years	18.946 (10.233-46.559) year ⁻¹
ρ	1 day - 10 years	0 (0-0) year ⁻¹
ϵ	1 day - 10 years	0 (0-0) year ⁻¹
m	0.186 (0.088-0.284) year ⁻¹	0.184 (0.119-0.274) year ⁻¹
m_j	0.500 (0.360-0.639) year ⁻¹	0.497 (0.352-0.633) year ⁻¹
c	-	12.58 (6.796-20.284)
s	130 (111-150)	129.048 (101.379-159.372)
ϕ	7.180 (6.787-7.571)	7.193 (6.992-7.41)
ω	1 day - 10 years	0 (0-0) year ⁻¹
ω_m	1.800 (1.41-2.19) year ⁻¹	1.795 (1.41-2.181) year ⁻¹
R_0	> 1	8.122 (5.059-11.291)
d	1-30	12.61 (3.136-28.712)
ζ_s	0-1	0.923 (0.811-0.986)
ζ_p	0-1	0.564 (0.407-0.754)
ζ_u	0-1	0.308 (0.068-0.8)
κ	4000 (2025-7867)	4308.783 (2228-8590)
c_ν	1	1
s_ν	-	8.388 (1.011-40.518)
ϕ_ν	-	0.581 (0.413-0.834)

¹ Table for model 6, SIR with seasonal force posterior estimates, 95% credible intervals are shown in brackets, model corresponds to model 6 in table SM1

Table 8: Model 7

Parameter	Prior	Posterior
γ	1 day - 10 years	4.123 (2.084-6.324) year ⁻¹
ρ	1 day - 10 years	0 (0-0) year ⁻¹
ϵ	1 day - 10 years	0 (0-0) year ⁻¹
m	0.186 (0.088-0.284) year ⁻¹	0.231 (0.143-0.31) year ⁻¹
m_j	0.500 (0.360-0.639) year ⁻¹	0.532 (0.409-0.677) year ⁻¹
c	-	16.541 (9.336-25.409)
s	130 (111-150)	130.062 (98.526-158.312)
ϕ	7.180 (6.787-7.571)	7.186 (7.028-7.353)
ω	1 day - 10 years	0.156 (0.002-0.49) year ⁻¹
ω_m	1.800 (1.41-2.19) year ⁻¹	1.832 (1.452-2.212) year ⁻¹
R_0	> 1	123.269 (73.495-149.935)
d	1-30	9.465 (1.18-27.194)
ζ_s	0-1	0.927 (0.839-0.987)
ζ_p	0-1	0.418 (0.265-0.588)
ζ_u	0-1	0.248 (0.038-0.826)
κ	4000 (2025-7867)	3854.169 (2158-8072)
c_ν	1	1
s_ν	-	0 (0-0)
ϕ_ν	-	0 (0-0)

¹ Table for model 7, SIRS with no seasonal force posterior estimates, 95% credible intervals are shown in brackets, model corresponds to model 7 in table SM1

Table 9: Model 8

Parameter	Prior	Posterior
γ	1 day - 10 years	11.329 (5.546-22.029) year ⁻¹
ρ	1 day - 10 years	0 (0-0) year ⁻¹
ϵ	1 day - 10 years	0 (0-0) year ⁻¹
m	0.186 (0.088-0.284) year ⁻¹	0.19 (0.052-0.291) year ⁻¹
m_j	0.500 (0.360-0.639) year ⁻¹	0.505 (0.362-0.64) year ⁻¹
c	-	12.72 (3.191-21.876)
s	130 (111-150)	129.432 (100.452-157.517)
ϕ	7.180 (6.787-7.571)	7.137 (6.949-7.332)
ω	1 day - 10 years	0.947 (0.084-2.46) year ⁻¹
ω_m	1.800 (1.41-2.19) year ⁻¹	1.797 (1.699-1.895) year ⁻¹
R_0	> 1	87.343 (44.169-149.329)
d	1-30	12.627 (2.547-28.565)
ζ_s	0-1	0.922 (0.822-0.985)
ζ_p	0-1	0.678 (0.459-0.88)
ζ_u	0-1	0.564 (0.19-1)
κ	4000 (2025-7867)	4655.028 (2535-9419)
c_ν	1	1
s_ν	-	30.441 (12.255-49.976)
ϕ_ν	-	2.147 (1.572-2.577)

¹ Table for model 8, SIRS with seasonal force posterior estimates, 95% credible intervals are shown in brackets, model corresponds to model 8 in table SM1

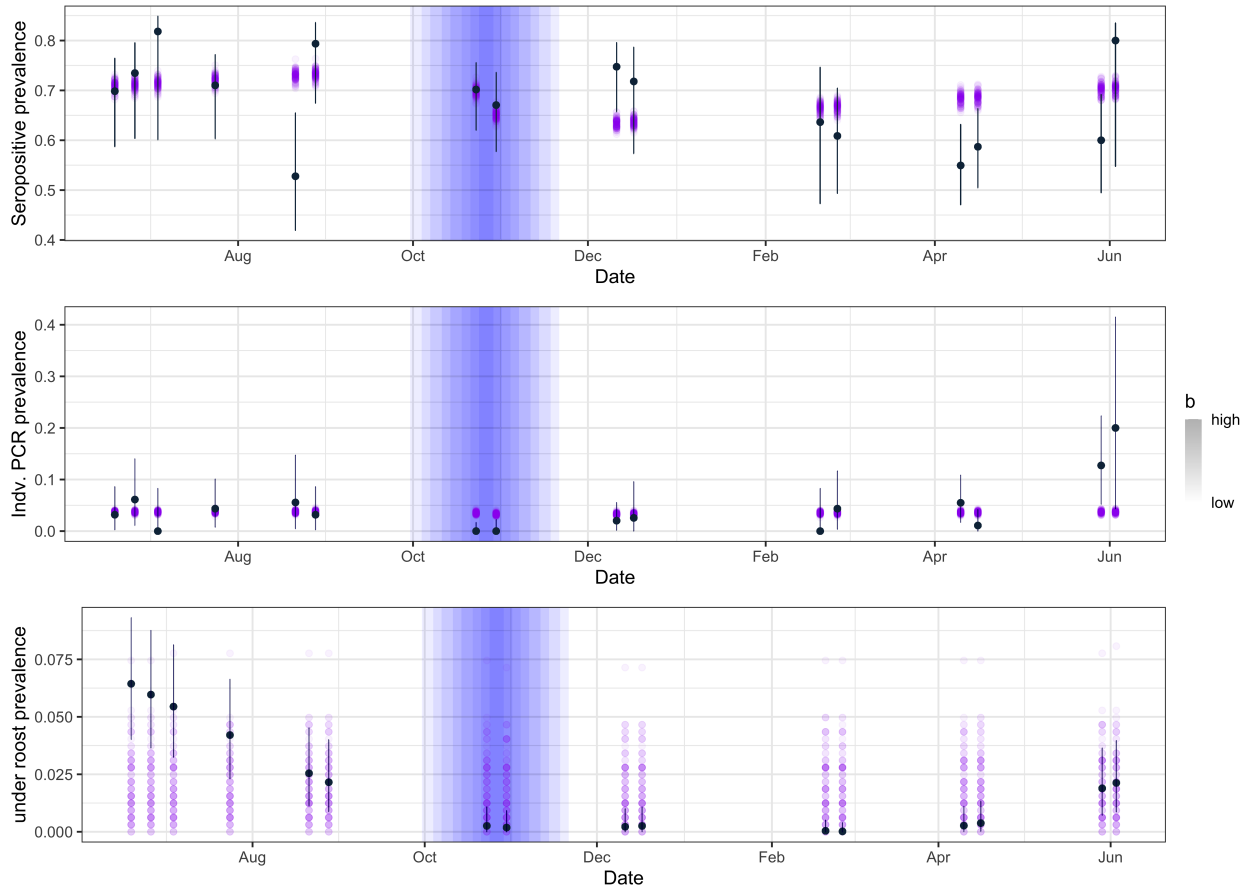


Figure 2: 100 repeat runs of the SILI model without seasonal forcing and without maternal immunity (model 1 in table 1), parameterised using the median values from the posterior estimates of each parameter. Dark blue points show the observed data, purple points show the model outputs for each run of the model at the corresponding observed time period. The top figure shows the simulated and observed serological prevalence, the middle figure shows the simulated and observed virus RNA prevalence from individual urine samples, and the bottom figure shows the simulated and predicted (using observed data and contributing bats parameter d) virus RNA prevalence from the under-roost samples. Confidence intervals on observed data are calculated as binomial confidence intervals, with a beta prior on the binomial distribution; the shape of the beta prior for individual samples is uninformative and for under-roost data is derived from the corresponding fitted overdispersion parameters for each data-type.

157
158
159
160
161
162

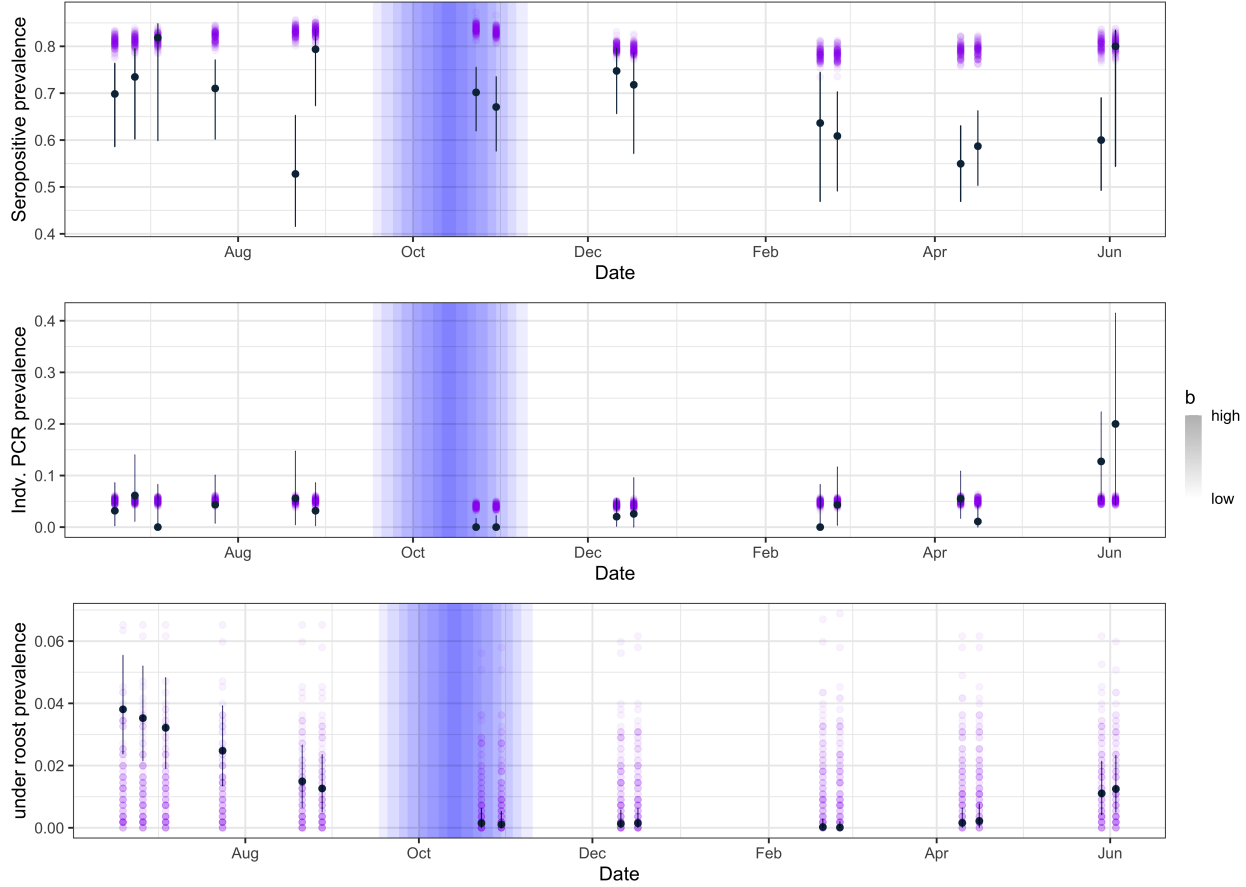


Figure 3: 100 repeat runs of the maternal immunity SILI model without seasonal forcing (model 2 in table 1), parameterised using the median values from the posterior estimates of each parameter. Dark blue points show the observed data, purple points show the model outputs for each run of the model at the corresponding observed time period. The top figure shows the simulated and observed serological prevalence, the middle figure shows the simulated and observed virus RNA prevalence from individual urine samples, and the bottom figure shows the simulated and predicted (using observed data and contributing bats parameter d) virus RNA prevalence from the under-roost samples. Confidence intervals on observed data are calculated as binomial confidence intervals, with a beta prior on the binomial distribution; the shape of the beta prior for individual samples is uninformative and for under-roost data is derived from the corresponding fitted overdispersion parameters for each data-type.

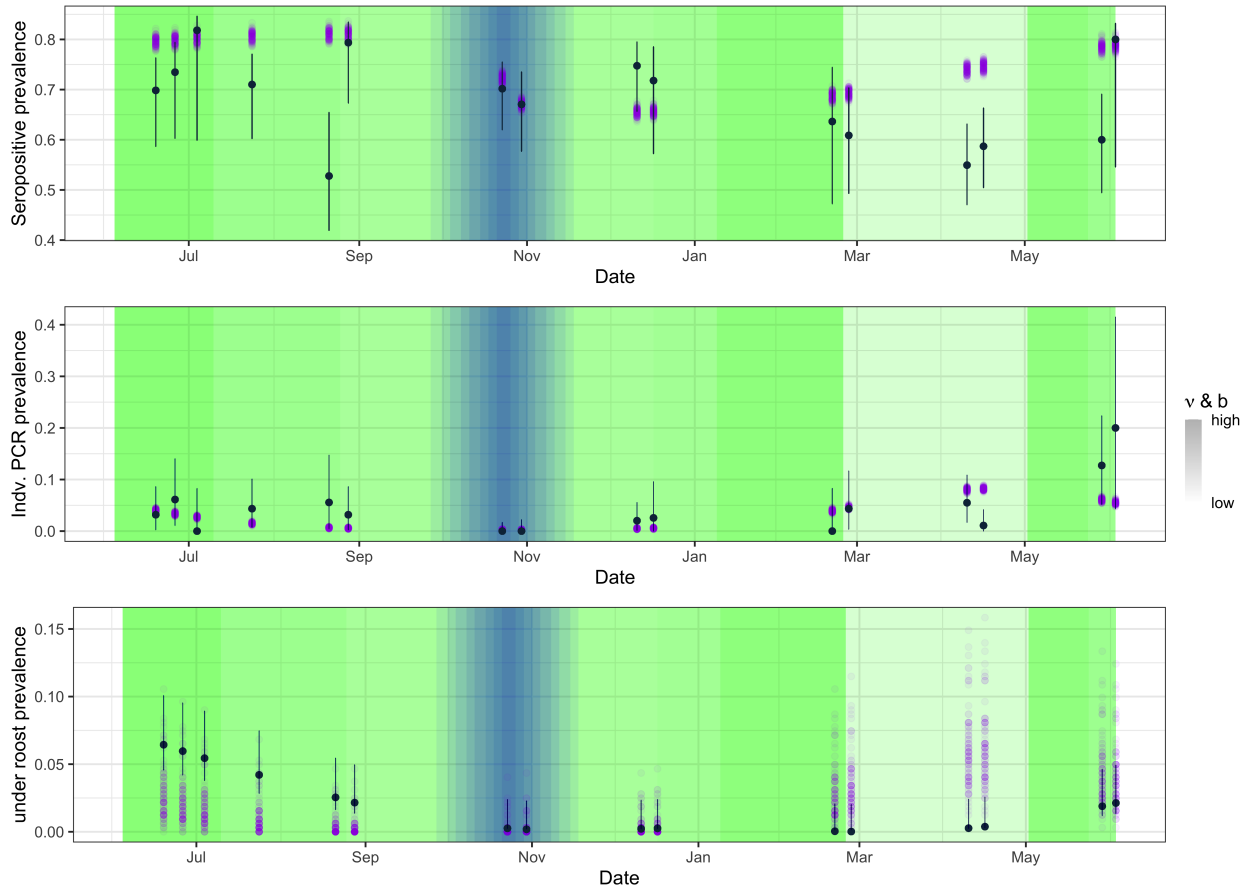


Figure 4: 100 repeat runs of the SILI model with seasonal forcing and without maternal immunity (model 3 in table 1), parameterised using the median values from the posterior estimates of each parameter. Dark blue points show the observed data, purple points show the model outputs for each run of the model at the corresponding observed time period. The top figure shows the simulated and observed serological prevalence, the middle figure shows the simulated and observed virus RNA prevalence from individual urine samples, and the bottom figure shows the simulated and predicted (using observed data and contributing bats parameter d) virus RNA prevalence from the under-roost samples. Confidence intervals on observed data are calculated as binomial confidence intervals, with a beta prior on the binomial distribution; the shape of the beta prior for individual samples is uninformative and for under-roost data is derived from the corresponding fitted overdispersion parameters for each data-type.

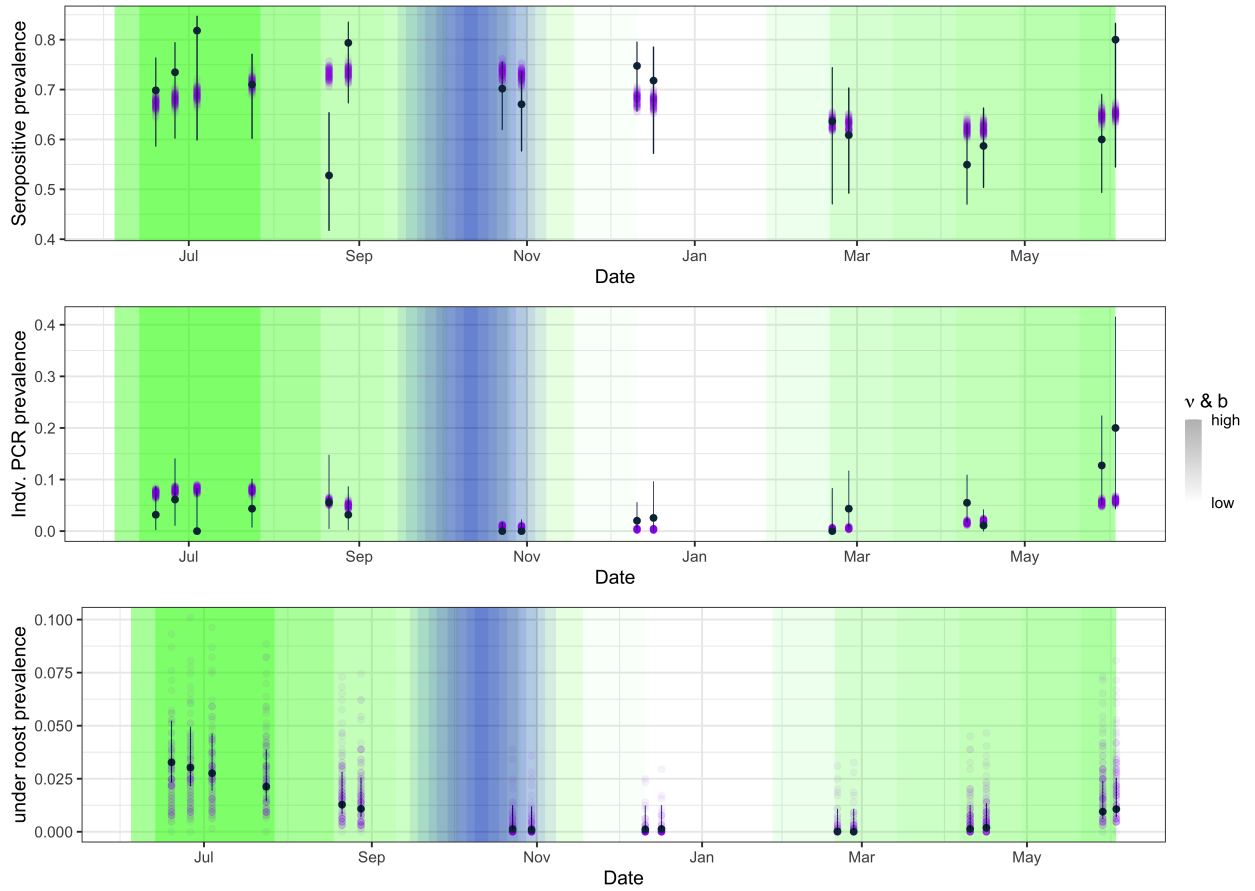


Figure 5: 100 repeat runs of the maternal immunity SILI model with seasonal forcing (model 4 in table 1), parameterised using the median values from the posterior estimates of each parameter. Dark blue points show the observed data, purple points show the model outputs for each run of the model at the corresponding observed time period. The top figure shows the simulated and observed serological prevalence, the middle figure shows the simulated and observed virus RNA prevalence from individual urine samples, and the bottom figure shows the simulated and predicted (using observed data and contributing bats parameter d) virus RNA prevalence from the under-roost samples. Confidence intervals on observed data are calculated as binomial confidence intervals, with a beta prior on the binomial distribution; the shape of the beta prior for individual samples is uninformative and for under-roost data is derived from the corresponding fitted overdispersion parameters for each data-type.

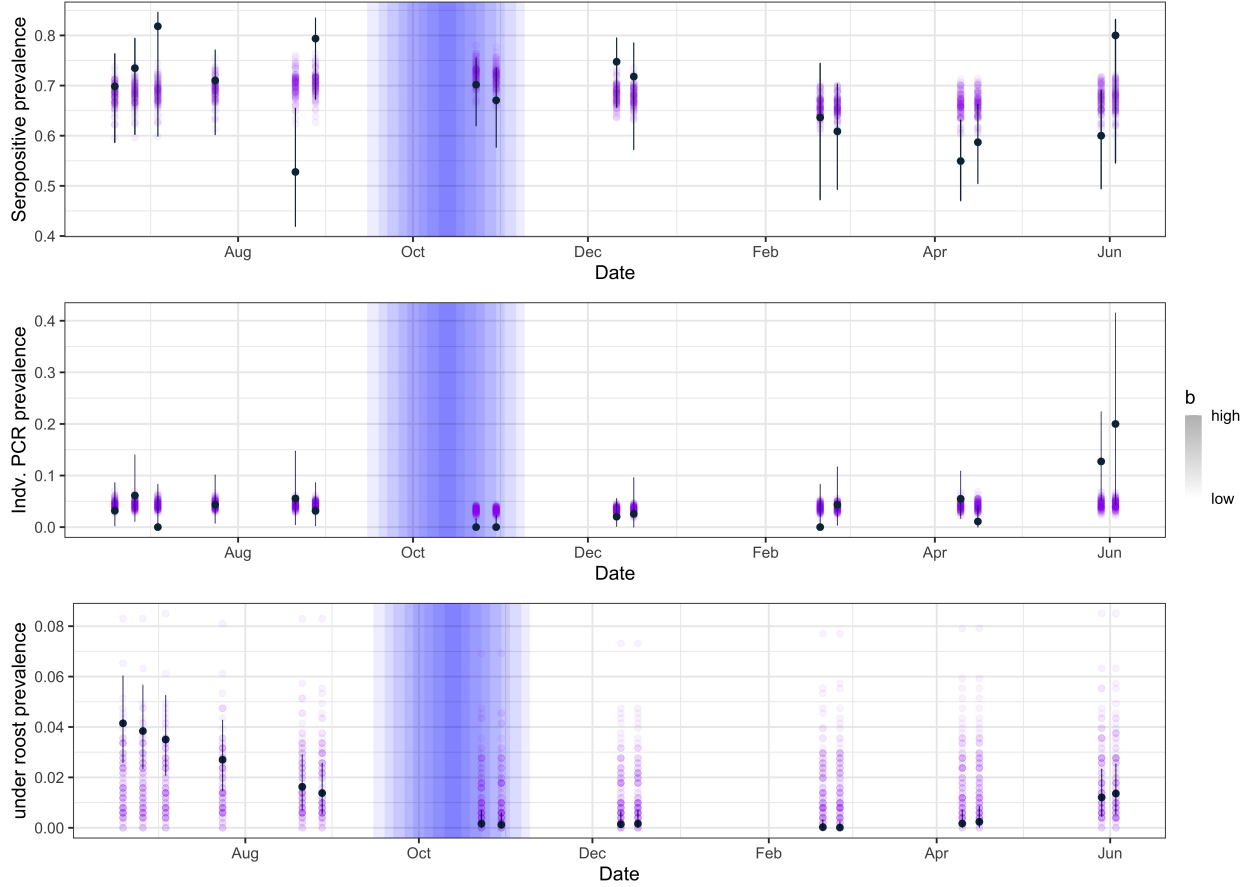


Figure 6: 100 repeat runs of the SIR model without seasonal forcing (model 5 in table 1), parameterised using the median values from the posterior estimates of each parameter. Dark blue points show the observed data, purple points show the model outputs for each run of the model at the corresponding observed time period. The top figure shows the simulated and observed serological prevalence, the middle figure shows the simulated and observed virus RNA prevalence from individual urine samples, and the bottom figure shows the simulated and predicted (using observed data and contributing bats parameter d) virus RNA prevalence from the under-roost samples. Confidence intervals on observed data are calculated as binomial confidence intervals, with a beta prior on the binomial distribution; the shape of the beta prior for individual samples is uninformative and for under-roost data is derived from the corresponding fitted overdispersion parameters for each data-type.

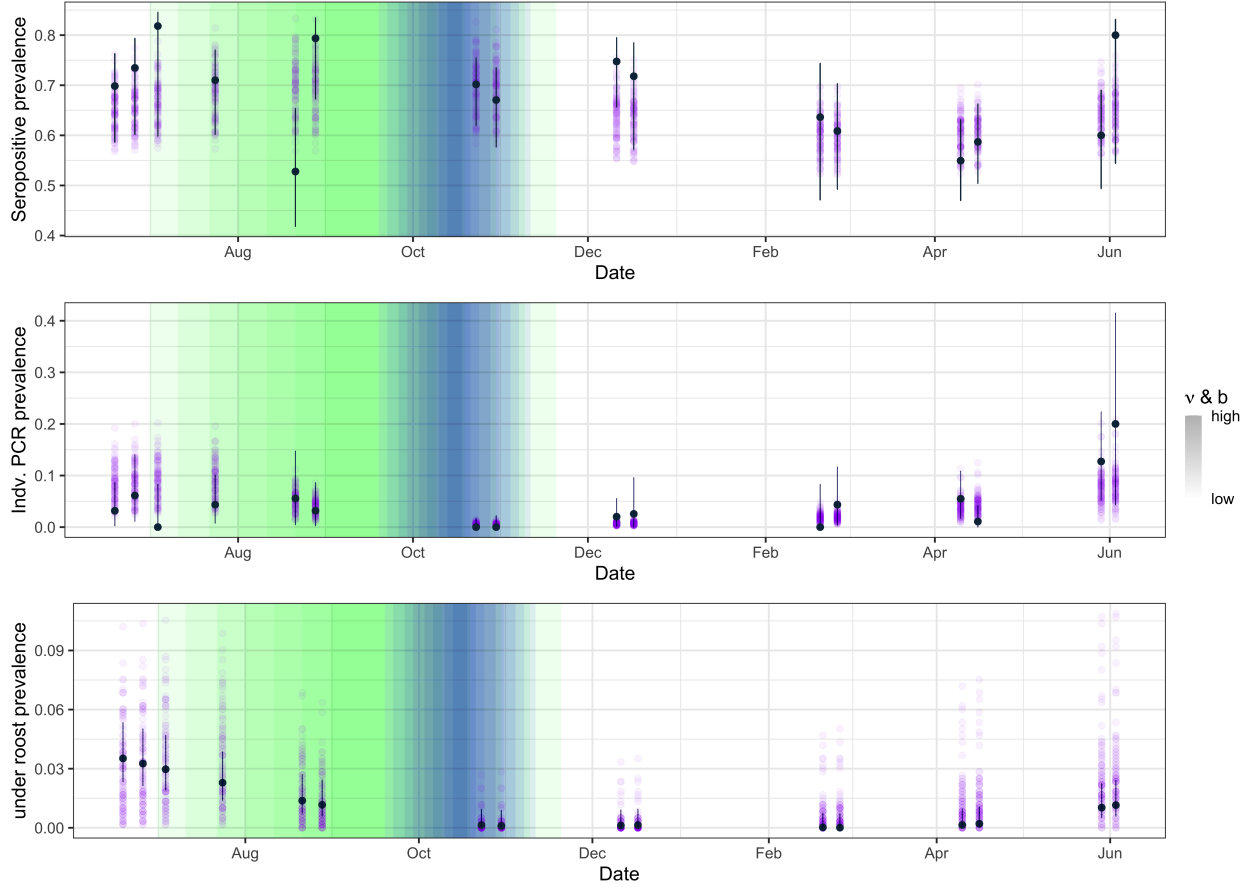


Figure 7: 100 repeat runs of the SIR model with seasonal forcing (model 6 in table 1), parameterised using the median values from the posterior estimates of each parameter. Dark blue points show the observed data, purple points show the model outputs for each run of the model at the corresponding observed time period. The top figure shows the simulated and observed serological prevalence, the middle figure shows the simulated and observed virus RNA prevalence from individual urine samples, and the bottom figure shows the simulated and predicted (using observed data and contributing bats parameter d) virus RNA prevalence from the under-roost samples. Confidence intervals on observed data are calculated as binomial confidence intervals, with a beta prior on the binomial distribution; the shape of the beta prior for individual samples is uninformative and for under-roost data is derived from the corresponding fitted overdispersion parameters for each data-type.

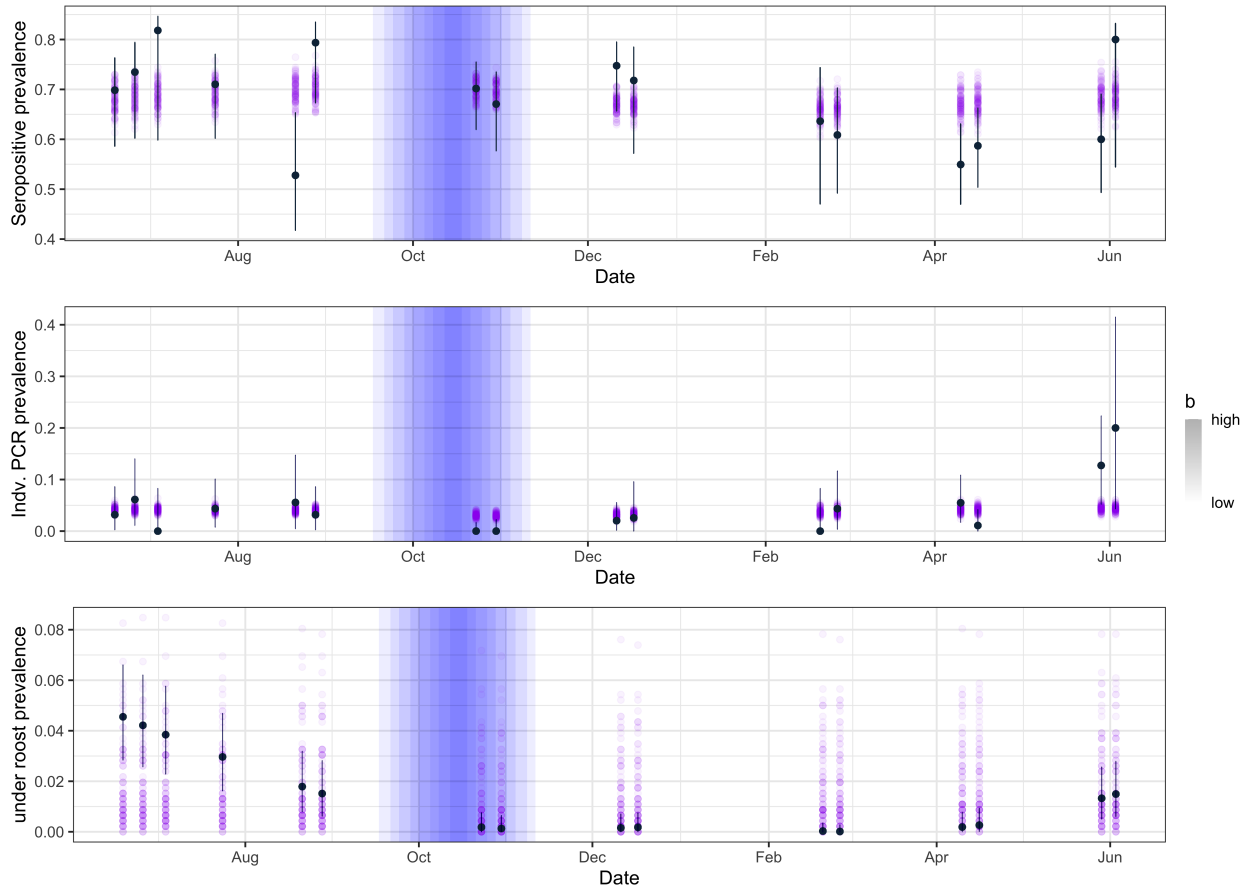


Figure 8: 100 repeat runs of the model without seasonal forcing (model 7 in table 1), parameterised using the median values from the posterior estimates of each parameter. Dark blue points show the observed data, purple points show the model outputs for each run of the model at the corresponding observed time period. The top figure shows the simulated and observed serological prevalence, the middle figure shows the simulated and observed virus RNA prevalence from individual urine samples, and the bottom figure shows the simulated and predicted (using observed data and contributing bats parameter d) virus RNA prevalence from the under-roost samples. Confidence intervals on observed data are calculated as binomial confidence intervals, with a beta prior on the binomial distribution; the shape of the beta prior for individual samples is uninformative and for under-roost data is derived from the corresponding fittedoverdispersion parameters for each data-type.

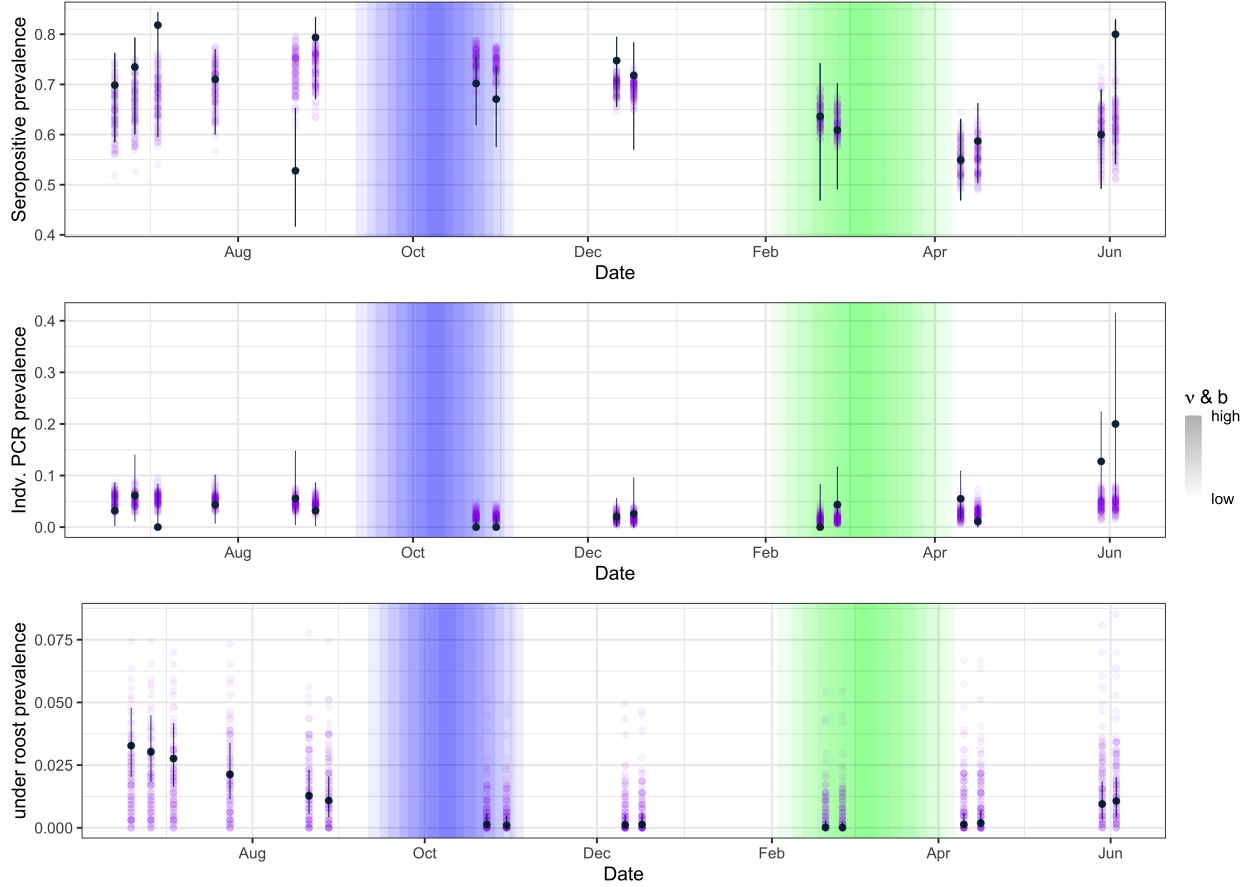


Figure 9: 100 repeat runs of the SIRS model with seasonal forcing (model 8 in table 1), parameterised using the median values from the posterior estimates of each parameter. Dark blue points show the observed data, purple points show the model outputs for each run of the model at the corresponding observed time period. The top figure shows the simulated and observed serological prevalence, the middle figure shows the simulated and observed virus RNA prevalence from individual urine samples, and the bottom figure shows the simulated and predicted (using observed data and contributing bats parameter d) virus RNA prevalence from the under-roost samples. Confidence intervals on observed data are calculated as binomial confidence intervals, with a beta prior on the binomial distribution; the shape of the beta prior for individual samples is uninformative and for under-roost data is derived from the corresponding fittedoverdispersion parameters for each data-type.

163 **References**

- 164 Andrieu, Christophe, Arnaud Doucet, and Roman Holenstein. 2010. “Particle Markov Chain Monte Carlo
165 Methods.” *Journal of the Royal Statistical Society: Series B (Statistical Methodology)* 72 (3): 269–342.
- 166 Chiang, Chin-long, and William C et al. Reeves. 1962. “Statistical Estimation of Virus Infection Rates in
167 Mosquito Vector Populations.” *American Journal of Hygiene* 75 (3).
- 168 Fasiolo, Matteo, Natalya Pya, Simon N Wood, and others. 2016. “A Comparison of Inferential Methods for
169 Highly Nonlinear State Space Models in Ecology and Epidemiology.” *Statistical Science* 31 (1): 96–118.
- 170 Kantas, Nikolas, Arnaud Doucet, Sumeetpal S Singh, Jan Maciejowski, Nicolas Chopin, and others. 2015.
171 “On Particle Methods for Parameter Estimation in State-Space Models.” *Statistical Science* 30 (3):
172 328–51.
- 173 Knape, Jonas, and Perry De Valpine. 2012. “Fitting Complex Population Models by Combining Particle
174 Filters with Markov Chain Monte Carlo.” *Ecology* 93 (2): 256–63.
- 175 Peel, Alison J, JRC Pulliam, AD Luis, RK Plowright, TJ O’Shea, DTS Hayman, JLN Wood, CT Webb,
176 and O Restif. 2014. “The Effect of Seasonal Birth Pulses on Pathogen Persistence in Wild Mammal
177 Populations.” *Proceedings of the Royal Society B: Biological Sciences* 281 (1786): 20132962.
- 178 Peters, Gareth W, Geoff R Hosack, and Keith R Hayes. 2010. “Ecological Non-Linear State Space Model Se-
179 lection via Adaptive Particle Markov Chain Monte Carlo (AdPMCMC).” *arXiv Preprint arXiv:1005.2238*.
- 180 Sheinson, Daniel M, Jarad Niemi, and Wendy Meiring. 2014. “Comparison of the Performance of Particle
181 Filter Algorithms Applied to Tracking of a Disease Epidemic.” *Mathematical Biosciences* 255: 21–32.
- 182 Smith, Adrian. 2013. *Sequential Monte Carlo Methods in Practice*. Springer Science & Business Media.